Materials Science and Engineering A 527 (2010) 5582–5591

Contents lists available at ScienceDirect

Materials Science and Engineering A

journal homepage: www.elsevier.com/locate/msea

Experimental and modeling investigation on SiC_p distribution in powder metallurgy processed SiC_p/2024 Al composites

Z.Y. Liu, Q.Z. Wang, B.L. Xiao*, Z.Y. Ma, Y. Liu

Shenyang National Laboratory for Materials Science, Institute of Metal Research, Chinese Academy of Sciences, 72 Wenhua Road, Shenyang 110016, China

ARTICLE INFO

Article history:
Received 15 March 2010
Accepted 4 May 2010

Keywords:
Analytical modeling
Metal-matrix composites
Powder metallurgy
Reinforcement distribution

ABSTRACT

SiC_p/2024Al composites were fabricated through the powder metallurgy (PM) technique. The mixing process was modified by using a high ball to charge ratio (BCR), which resulted in improved homogeneity of the SiC_p distribution, as well as enhanced tensile strengths of the as-pressed composites. A small particle size ratio of aluminum to SiC_p (PSR) and extrusion also improved the uniformity of the SiC_p distribution. The improvements by the three approaches were quantitatively analyzed using a critical volume fraction model. The model demonstrates that a small PSR and a large deformation ratio of aluminum particles were two essential factors of improving the homogeneity of the SiC_p. A homogeneity analysis using the Dirichlet Tessellation method provided an additional explanation for the model.

1. Introduction

SiC particulate (SiC_p) reinforced Al matrix composites are powerful candidates in the automobile and aerospace industries [1–5]. Control of the SiC_p distribution in the Al matrix is an important technique, since clustering degrades the tensile properties of the composites [6–15]. In powder metallurgy (PM) SiC_p/Al composites, SiC_p agglomeration or necklace structure might be produced in the case of a large volume fraction of SiC_p or a large particle size ratio (PSR) of Al to SiC_p [13–17]. Enhancing the mixing process [18–21], properly selection of the PSR [13–17] and performing a post-fabrication deformation such as extrusion [22] are the most common methods of improving the homogeneity distribution. However, the principles which are responsible for the improvement have not been well understood.

In order to guide the fabrication and secondary processing of the composites, it is necessary to build a criterion for evaluating the homogeneity of the reinforcement distribution. Some critical volume fraction models of reinforcement [14,16] have been built to describe the influences of the PSR and the volume fraction (V_f) on the homogeneity of the reinforcement distribution. If the volume fraction of the reinforcement exceeded the critical volume fraction, a non-homogeneous distribution of the reinforcement would appear. Bhanu Prasad et al. [16] set up a clustering probability map of the reinforcement for the as-pressed or as-sintered composites in view of geometrical location. Slipenyuk et al. [14] set up a critical volume fraction model based on the as-extruded SiC_p/Al composites. However, the above models could only be suited for one process, either the hot-press process or the extrusion process. Furthermore, the critical volume fraction on the deformation of Al powders during mixing process was seldom discussed. Therefore, a critical volume fraction model considering the deformation of Al powder and PSR during different processes is highly desirable.

In this article, the effects of modified mixing processes with a high ball to charge ratio, extrusion and PSR, respectively on the homogeneity of SiC_p distribution were investigated. A critical volume fraction model was proposed to quantitatively evaluate the homogeneity of the distribution. Furthermore, the reinforcement distribution associated with the PSR, mixing process and extrusion were also analyzed by the Dirichlet Tessellation method [12,23].

2. Experimental procedure

2.1. Materials and mixing process

The as-received 2024Al and α-SiC powders were spherical and polygonal shaped, respectively. 2024Al had a nominal composition of Al–4.5%Cu–1.5%Mg (wt.%). In order to investigate the effects of the ball to charge ratio (BCR), extrusion and the PSR on the homogeneity of SiC_p and mechanical properties of the composites, three groups of samples were fabricated (Table 1).

In the first group of samples, the composite powders were mixed for 12 h. For comparison, the powders mixed for 1, 4 and 8 h were also withdrawn. For convenience, the powders or the composites under BCR of 1:1 and 10:1 were labeled as BCR1 and BCR10, respectively. In the second group of samples, the experiment aimed at

* Corresponding author. Tel.: +86 24 839 786 30; fax: +86 24 239 717 49.
E-mail address: blxiao@imr.ac.cn (B.L. Xiao).

0921-5093/$ – see front matter.
doi:10.1016/j.msea.2010.05.006

Table 1
Materials and process parameters used in mixing.

Experiment	D_{SiC} (μm)[a]	D_{Al} (μm)[a]	SiC vol.%	Ball to charge ratio (BCR)	Mixing time (h)
Group 1	3.5	13	15	1:1	12
			15, 20	10:1	
Group 2	7	29	5, 10, 15, 20	1:1	8
Group 3	3.5	3, 5, 7, 13, 29	15	1:1	8

[a] D_{SiC} and D_{Al} are diameters of SiC and Al powders, respectively.

investigating the effect of extrusion on the critical volume fraction and homogeneity of the SiC_p distribution in the composites. In order to investigate the PSR effect on the distribution of the SiC_p, in the third group of samples, 15 vol.% SiC_p/2024Al powders were prepared by fixing the size of the SiC_p and changing the size of the Al powders. For all samples, the SiC powders were dried in a furnace at 423 K for 5 h and then mixed with the Al powders in a bi-axis rotary mixer with a rotation speed of 50 rpm. No process control agent was added.

2.2. Fabrication of composite

The as-mixed powders were cold pressed in a die, degassed and then hot-pressed in vacuum under a pressure of 80 MPa. The as-pressed composites in the first group were solutionized at 768 K for 1 h, water quenched and then naturally aged for 96 h. The as-pressed billets in the second and third groups were hot extruded into rods at 723 K at an extrusion ratio of 9:1. The extruded rods were heat treated with the same procedure as the samples in the first group.

2.3. Microstructure and mechanical properties

Morphologies of the as-mixed powders were observed by scan electron microscopy (SEM, SSX-550). The SiC_p distribution in the as-mixed powders, the as-pressed and as-extruded composites were observed by optical microscopy (OM, Axiovert 200 MAT). Density of each of the composites was measured using the Archimedean principle. Room temperature tensile tests were performed at a strain rate of 0.001 s^{-1} on an AG-100kNG tester. Tensile specimens with a gauge diameter of 5 mm and gauge length of 20 mm were machined from the heat treated samples.

3. Results

3.1. Microstructure of SiC_p/2024Al composite powders

The morphology of the composite powders mixed for 12 h with different BCRs in the first group of samples are shown in Fig. 1. For the BCR1 powders, the Al particles remained spheroidal and the SiC_p were freely distributed at the periphery of the Al particles. However, for the BCR10 powders, the composite powders displayed an irregular morphology, indicating that they underwent severe deformation during mixing.

Fig. 2 shows the evolution of the morphology of the BCR10 composite powders mixed for 1, 4, 8 and 12 h. For the 1 h sample, the Al particles remained in spheroidal shape, and the SiC_p were found mainly among the spheroidal Al particles. After being mixed for 4 and 8 h, the Al particles were transformed from spheroidal shape to flaky shape. In addition, many SiC particles were enclosed between the flaky particles when they were aggregated into lamellar structures through cold welding (Fig. 2(b) and (c)). The width of a single flake in the lamellar particles, measured using the linear intercept method, was about 3–5 μm. When mixed for 12 h, almost all of the SiC particles were enclosed into the lamellar particles. The powders turned nearly equiaxial, implying that a balance between cold welding and fracture was built. The evolution of the morphology indicates that the low energy mixing using high BCR behaved a similar process as the high energy ball mill [18–21].

3.2. Microstructure of SiC_p/2024Al composites

Fig. 3 shows the optical micrographs of the as-pressed 15 vol.% and 20 vol.% SiC_p/2024Al composites in the first group of samples. The SiC_p in the BCR1 composite with concentration of 15 vol.% showed obvious necklace structure. Similar observations were found in previous studies [15–16]. For the BCR10 composite with concentration of 15 vol.%, a streamline-like distribution of SiC_p was observed and the SiC_p were more homogeneous (Fig. 3(b)). It indicates that a large BCR could improve the uniformity of the SiC distribution. However clusters appeared in the 20 vol.% SiC_p/2024Al even with a high BCR of 10:1 (Fig. 3(c)).

Fig. 4 shows the microstructure of the second group of composites. Similar to the observations of the BCR1 samples in the first group, the SiC_p were found at the periphery of the Al particles in the as-pressed composites. For the composites with volume fractions of 5 and 10 vol.%, the SiC_p were relatively homogeneous (Fig. 4(a) and (b)). However, clusters appeared at higher volume fractions of 15 and 20 vol.%, due to the inadequate specific surface area of the Al particles (Fig. 4(c) and (d)). Compared with that in

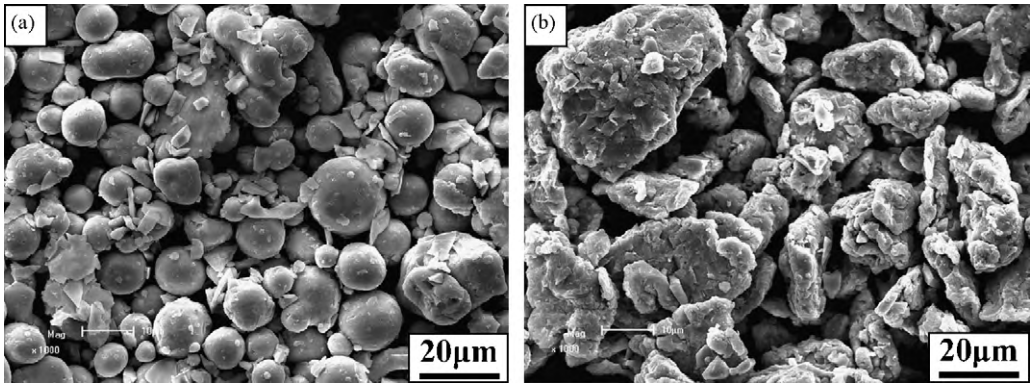

Fig. 1. SEM images of composite powders (group 1) mixed at ball to charge ratio of (a) 1:1 and (b) 10:1.

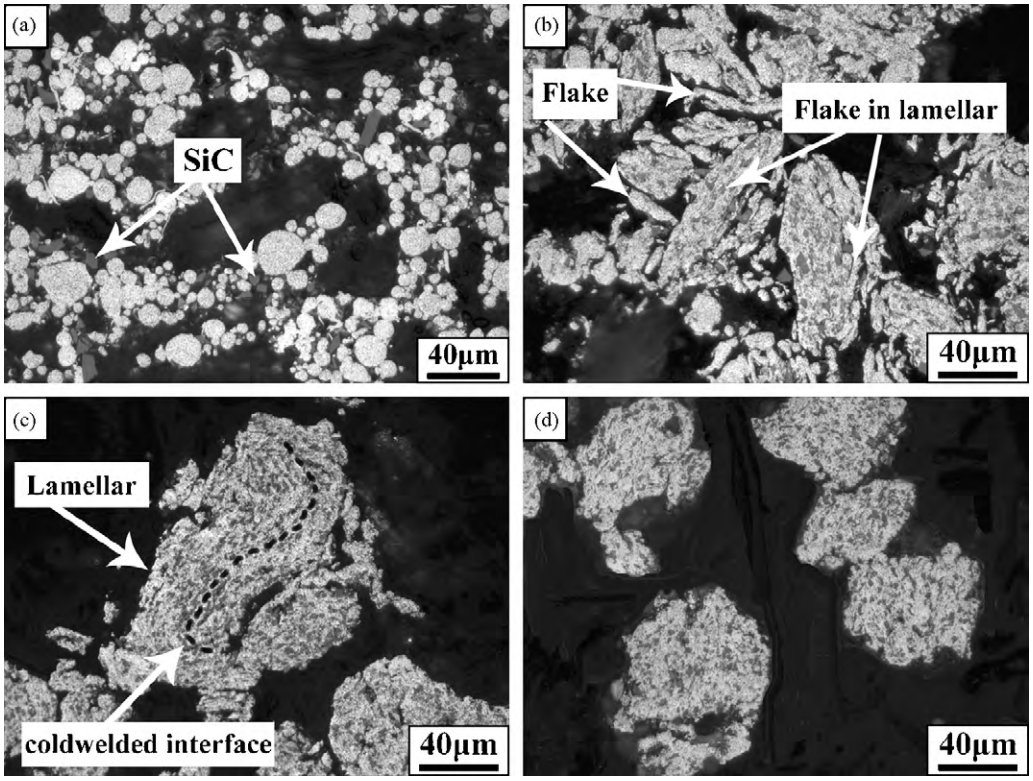

Fig. 2. Optical micrographs of composite (group 1) powders mixed at 10:1 ball to charge ratio for (a) 1 h, (b) 4 h (c) 8 h, and (d) 12 h. Dashed line in (c) referred to interfaces and streamline direction of SiC distribution in cold-welded lamellar structure.

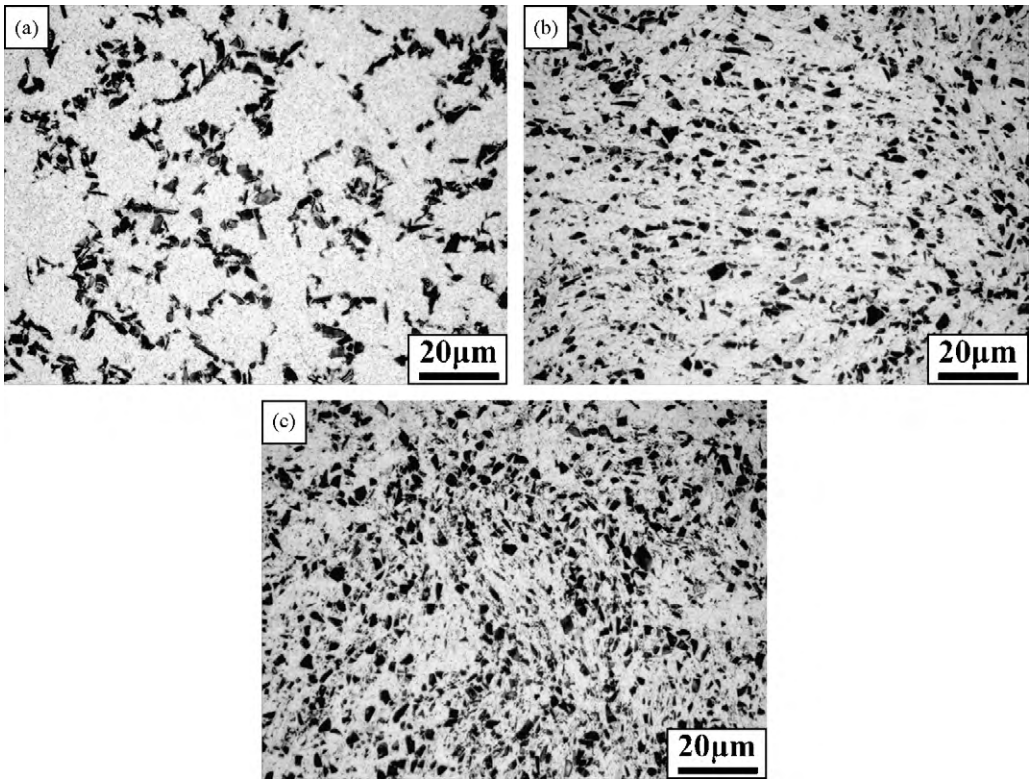

Fig. 3. Microstructure of various composites in group 1: (a) 1:1 BCR, 15 vol.% SiC; (b) 10:1 BCR, 15 vol.% SiC; (c) 10:1 BCR, 20 vol.% SiC.

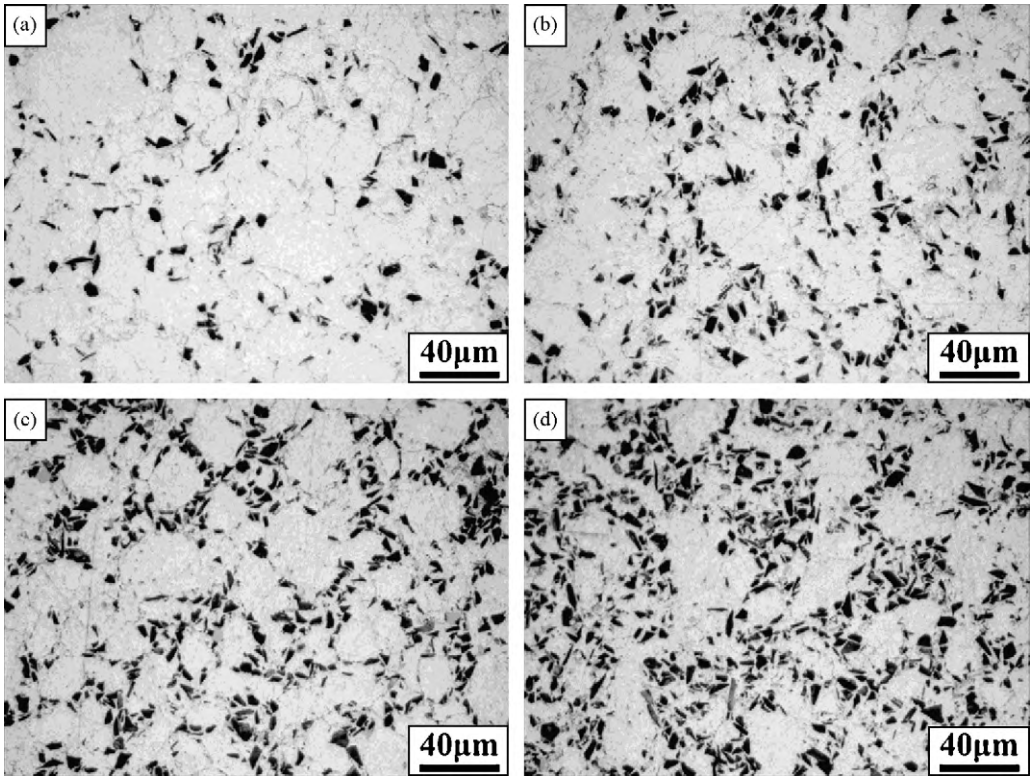

Fig. 4. Microstructure of as-pressed SiCp/2024Al composites (group 2) with SiC volume fraction of (a) 5%, (b) 10%, (c) 15%, and (d) 20%.

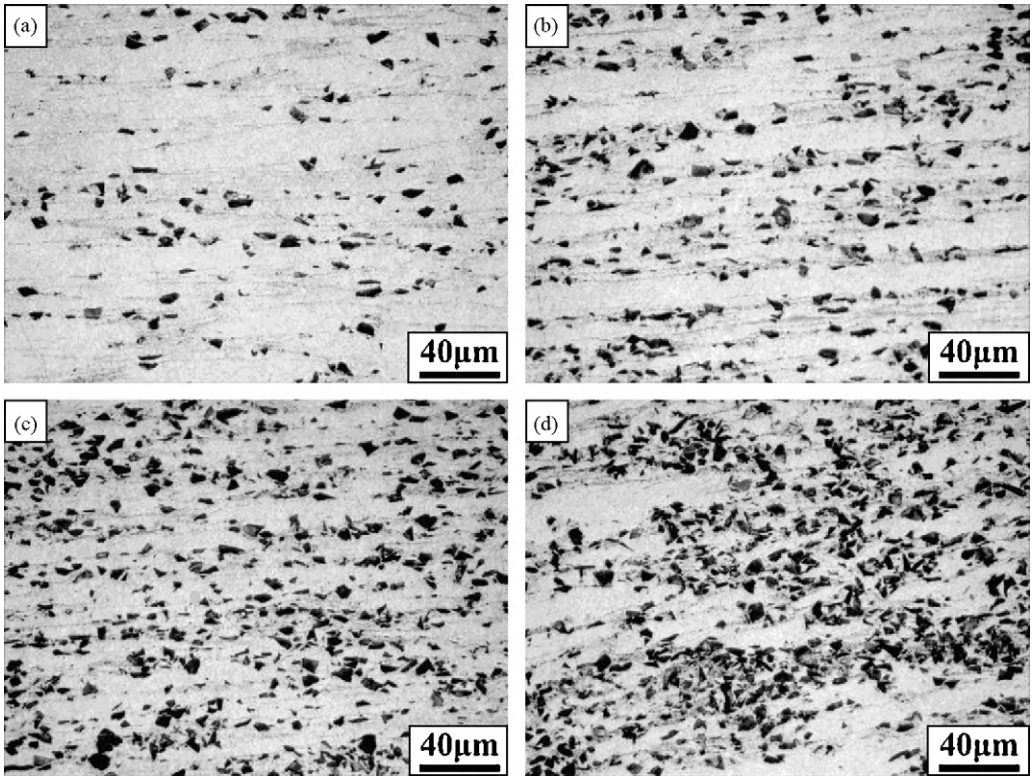

Fig. 5. Microstructure of as-extruded SiCp/2024Al composites (group 2) with particle volume fraction of (a) 5%, (b) 10%, (c) 15%, and (d) 20%. The extrusion direction is horizontal.

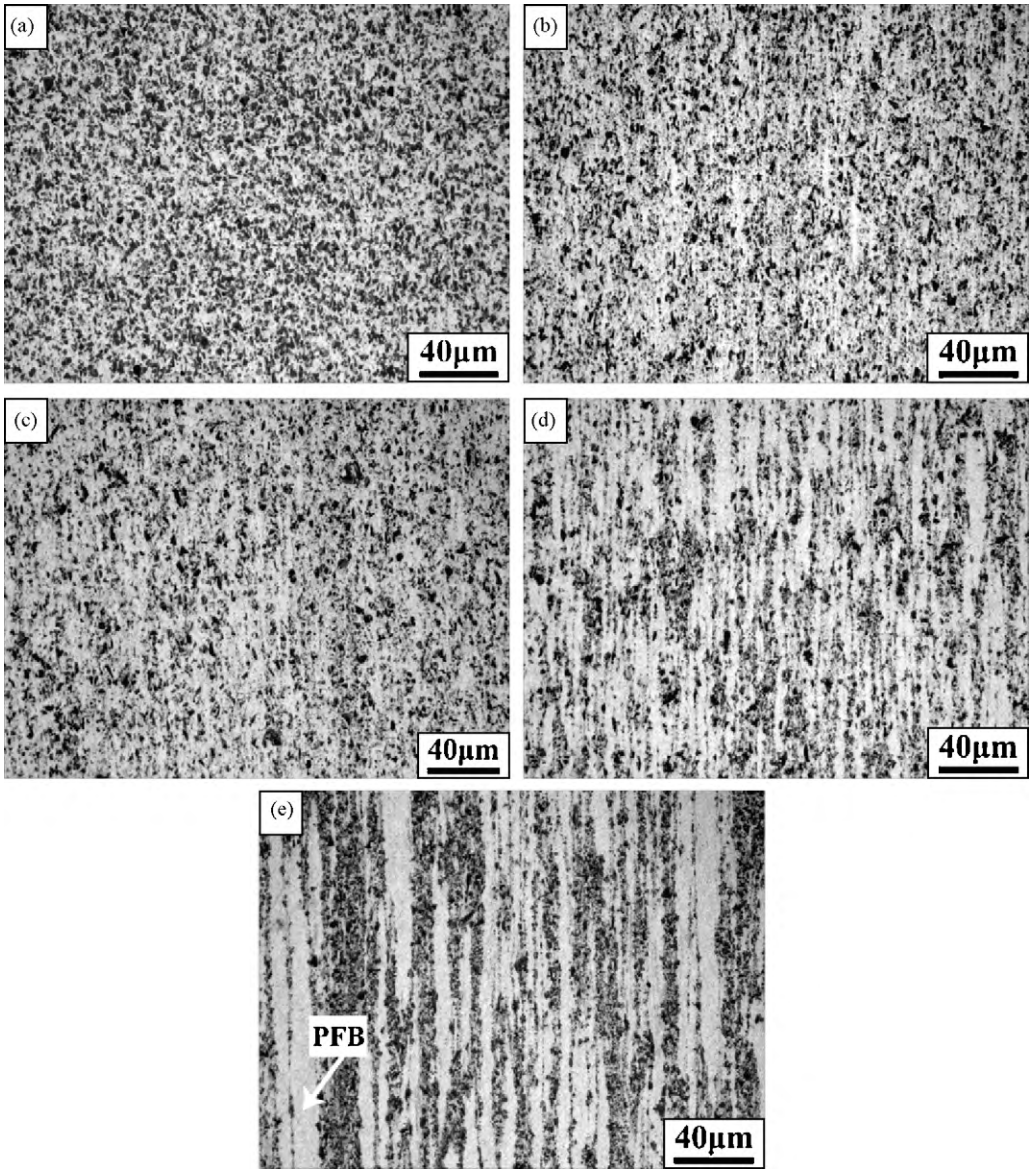

Fig. 6. Microstructure of as-extruded 15 vol.% SiCp/2024Al composites (group 3) with PSRs of (a) 0.86, (b) 1.43, (c) 2, (d) 3.7, and (e) 8.0. The extrusion direction was vertical.

the as-pressed composite, the distribution of the SiC_p in the as-extruded composite exhibited significant improvement (Fig. 5). The SiC_p were distributed along the extruding direction and the necklace distribution of the SiC_p disappeared. Obvious SiC clusters only were found in the 20 vol.% SiC_p/2024Al composite. By comparison, obvious clusters appeared in the as-pressed 15 vol.% SiC_p/2024Al composite (Fig. 4), which implies that extrusion could increase the critical volume fraction.

SiC distributions of the as-extruded composites in the third group of samples are shown in Fig. 6. A larger PSR led to a more non-homogeneous SiC distribution. Particle free bands (PFBs) were the main characteristics at large PSRs, which means that the SiC_p were densely distributed parallel to the extruding direction at large PSRs, resulting in a non-homogeneous distribution of the SiC_p.

3.3. Mechanical properties of SiC_p/2024Al composite

The mechanical properties of the 15 vol.% SiC_p/2024Al composite under two different BCRs are given in Table 2. High BCR increased both yield strength (YS) and ultimate tensile strength (UTS), due to a more homogeneous distribution. However, the elongation showed no improvement, due to weak interfacial bonding between Al–Al powders in the as-pressed composites. Furthermore, the improvement in UTS was larger than that in YS, which demonstrates that UTS was more sensitive to the distribution of SiC_p than YS.

Fig. 7 shows the mechanical properties and densities of the samples in group 2. The addition of SiC_p led to a linear increase of the composites density as long as the SiC_p were uniformly distributed in the matrix. However, the density of the composite with 20 vol.% reinforcements deviated from the Rule of Mixtures (ROM) (Fig. 7(a)), which also demonstrates the clustering. The YS increased as the SiC volume fraction was increased from 5 to 20 vol.%, whereas the UTS decreased when the SiC_p volume fraction reached up to 20 vol.%. However, a previous study [5] reported that both YS and UTS increased when SiC volume fraction was increased up to 25%.

Table 2
Tensile properties of composites (group 1) under different ball to charge ratio.

BCR	YS (MPa)	UTS (MPa)	Elongation (%)
1:1	379 ± 1	439 ± 2	0.8
10:1	385 ± 1	461 ± 5	0.8

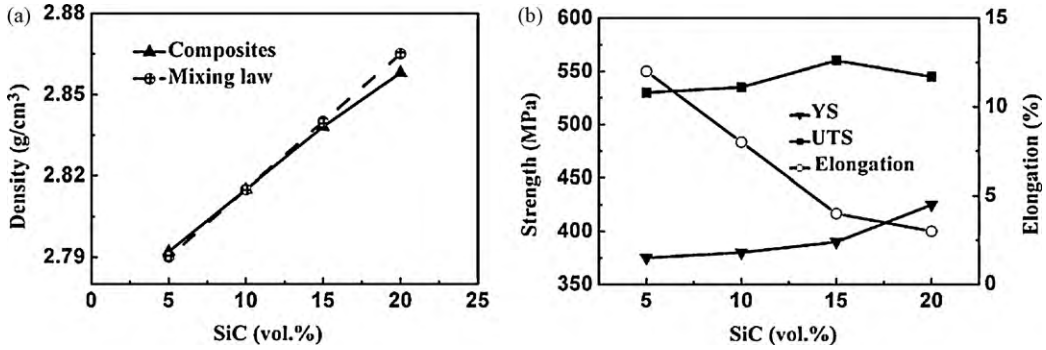

Fig. 7. Variation of (a) density and (b) tensile properties with SiC volume fraction for SiCp/2024Al composites in group 2.

The reason was attributed to the formation of clusters in the present composites. On one hand, voids might exist in clusters, which act as microcrack sources. On the other hand, reinforcement clusters induced stress concentration and accelerated the propagation of cracks [13–14]. Elongation decreased as the SiC content was increased, which resulted from higher triaxial stress state caused by the increase of clusters and the reduction of the interparticle distance.

Fig. 8 shows the effect of the PSR on the mechanical properties of 15 vol.% SiC_p/2024Al in the third group. A clear increasing trend in the tensile strength and significantly improved ductility as the PSR was decreased could be observed. This was attributed to a more homogeneous distribution of SiC_p [13,14,16]. Prasad [15] correlated the UTS of the as-pressed composite with the PSR by using an equation $y = a - b \ln x$. In this article, the mechanical properties of the as-extruded composites and the PSR ratio data are fitted into similar curves, as shown in Fig. 8. The tensile property data can be approximately fitted into straight lines with logarithm of PSR.

4. Modeling and discussion

As mentioned before, there was a critical volume fraction of reinforcement in the PM processed particle reinforced composites, above which the reinforcement cluster would appear. Further, for a constant volume fraction of the reinforcement, we hypothesized that a large critical volume fraction led to a more homogeneous distribution of the reinforcement. In order to determine this critical volume fraction, we supposed that all Al particles were separated from each other by continuous distribution of reinforcements. For the mixing and extrusion processes, the critical volume fractions were determined respectively.

4.1. Lamellar distribution in as-pressed composite

According to the evolution history of powder morphology, a simplified model is built to explain the powder evolution by using high BCR, as shown in Fig. 9.

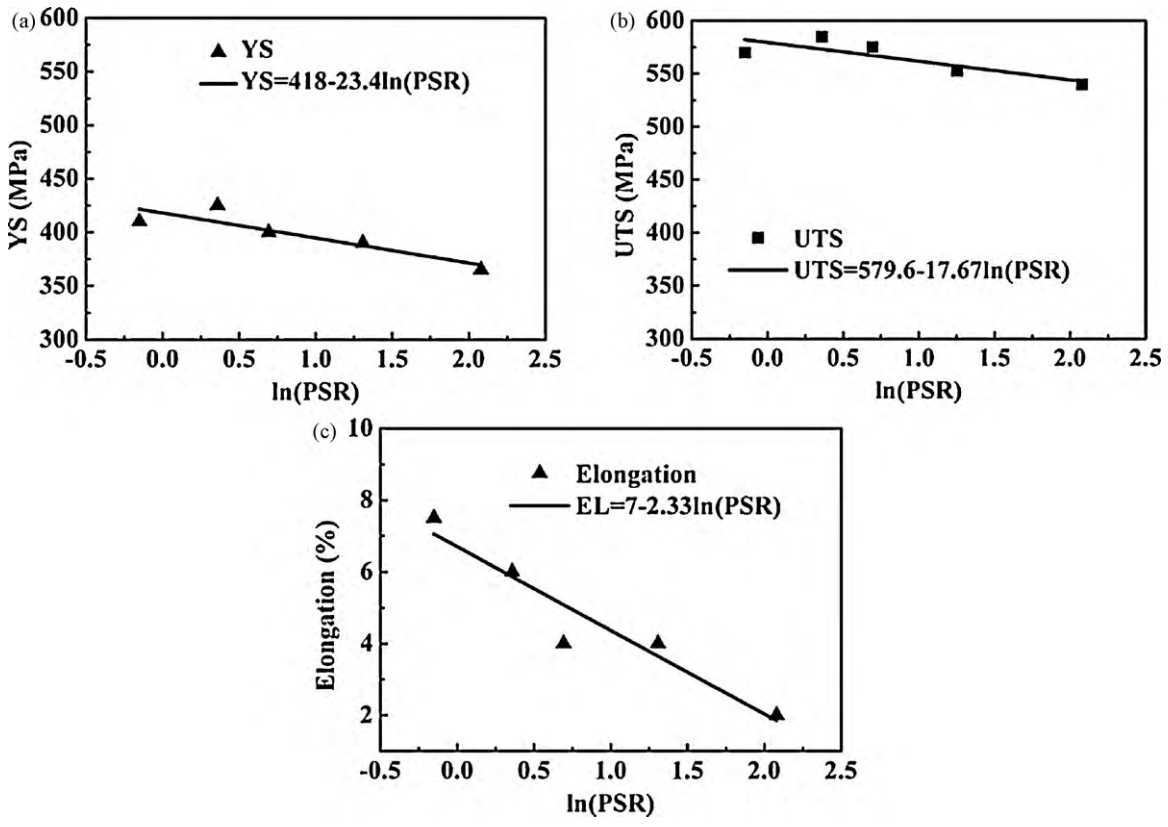

Fig. 8. Effect of PSRs on tensile properties of 15 vol.% SiCp/2024Al composites (group 3).

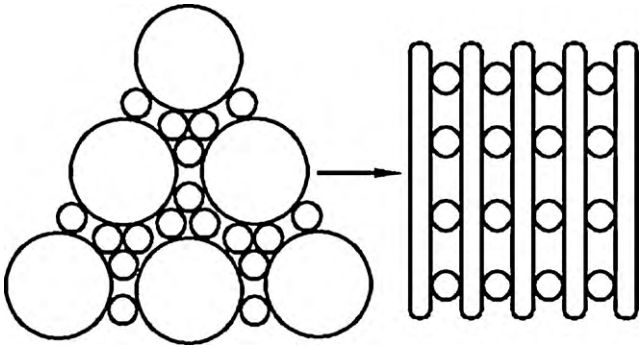

Fig. 9. Schematic of powder evolution during mixing using high ball to charge ratio. Small circles represent SiC particles while large circles represent aluminum particles, the rod represents the deformed aluminum particles after mixing.

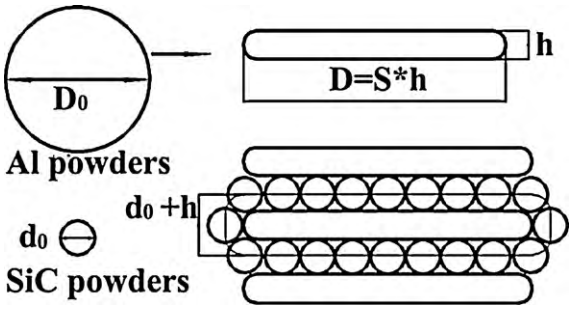

Fig. 10. Schematic of basic lamellar model with large ball to charge ratio.

Prior to the calculation, a series of simplifications are made:

(a) Volume change or fracture of the Al particles do not happen. Deformation and cold welding dominate the morphology evolution process. Once the cold welding happens, the width of the flaky Al particles in the lamellar structure will not change.
(b) After mixing, the shape of Al particle changes from spheroid to regular round disc.

In the lamellar structure, the SiC_p were fixed between the flaky aluminum particles during the cold welding process and the lamellar particles were randomly oriented in the mixture. So the critical volume fraction of SiC_p in the lamellar structure is considered equal to that in the composite.

The geometric model is shown in Fig. 10. According to the assumption of constant volume of the aluminum particle, we can obtain:

$$\frac{4}{3}\pi\left(\frac{D_0}{2}\right)^3 = \frac{1}{4}\pi D^2 h \tag{1}$$

where D_0 is the diameter of the Al particles, D and h are the diameter and height of the disc shaped Al particles after mixing, respectively. S is defined as the ratio of diameter to height of the disc shaped Al particles, namely:

$$S = \frac{D}{h} \tag{2}$$

In the lamellar structure, a basic lamellar unit, as shown by a continuous thin line in Fig. 10, is chosen for calculation. The volume of one Al particle is:

$$V_{Al} = \frac{h\pi D^2}{4} \tag{3}$$

And the volume of reinforcements per Al particle is:

$$V_{SiC} = \frac{(d_0+h)\pi(D+d_0)^2}{4} - \frac{h\pi D^2}{4} \tag{4}$$

where d_0 is the size of the SiC_p.

So the critical volume fraction of the reinforcement is:

$$V_{critical} = \lambda\frac{V_{SiC}}{V_{Al}+V_{SiC}} = \lambda\frac{(d_0+h)\pi(D+d_0)^2/4 - h\pi D^2/4}{(d_0+h)\pi(D+d_0)^2/4}$$
$$= \lambda\left(1 - \frac{0.667(D_0/d_0)^3}{(1+0.874S^{-2/3}D_0/d_0)(1+0.874S^{1/3}D_0/d_0)^2}\right) \tag{5}$$

where $\lambda(\lambda<1)$ is the maximum filling rate of the SiC_p in the homogenous composites and is considered to be constant; D_0/d_0 is the PSR of Al to SiC_p.

If the SiC_p fractured during mixing, the mean size of the SiC_p after mixing d_0 should replace d_0. Substituting a fracture ratio $\eta = d_0/d_0$ into Eq. (5) changes it to:

$$V_{critical} = \lambda\left(1 - \frac{0.667(\eta D_0/d_0)^3}{(1+0.874S^{-2/3}\eta D_0/d_0)(1+0.874S^{1/3}\eta D_0/d_0)^2}\right) \tag{6}$$

Eq. (6) indicates that the critical volume fraction is only dependent on S and PSR if the SiC_p fracture is ignored.Calculated by Eq. (6),

$$\frac{\partial(V_{critical})}{\partial(S)} > 0 \ (S>1); \quad \frac{\partial(V_{critical})}{\partial(PSR)} < 0 \tag{7}$$

According to Eq. (7), if S were large enough or PSR small enough, the critical volume fraction of reinforcement would obtain a large value. It means that a good SiC_p distribution would be obtained.

In the first group of samples, the PSR was equal to 4. At the lower BCR of 1:1, the shape of the Al particle was almost unchanged, thus the S was considered as 1. The $V_{critical}$ was considered to be 0.15 (Fig. 6), substituting these value to Eq. (6) yielded $\lambda = 0.27$.

For a BCR of 10:1, the width of the flaky Al particles (h) in the lamellar particles was about 5 μm. The value of S was calculated to be 4 while the value of h was input into Eqs. (1) and (2). Substituting the value of PSR and S into Eq. (6) yielded $V_{critical} = 17\%$. Namely, if the volume fraction of SiC_p was larger than 17 vol.%, clusters would appear. The 20 vol.% SiC_p/2024Al under BCR10 showed obvious clusters (Fig. 3(c)), which was in agreement with the criteria that if the volume fraction was larger than $V_{critical}$, non-homogeneous distribution would be produced.

4.2. Rod distribution in as-extruded composite

Slipenyuk et al. [14] used a model to calculate the $V_{critical}$ of the reinforcement during composite extrusion, and it assumed that the morphology of the aluminum particle was cubic morphology and changed to square bar after extrusion. However, that actual was that the morphology of aluminum particle was spherical. Considering the differences between assumption and reality, the model was modified by considering that the aluminum powder changed from actual spherical shape to round bar shape for higher accuracy. And then it is applied to our situation (Fig. 11). The $V_{critical}$ calculation is conducted based on the following simplifications:

(a) The SiC_p and Al in the as-pressed composite are packed in the same way as that in the as-mixed composite powders. The

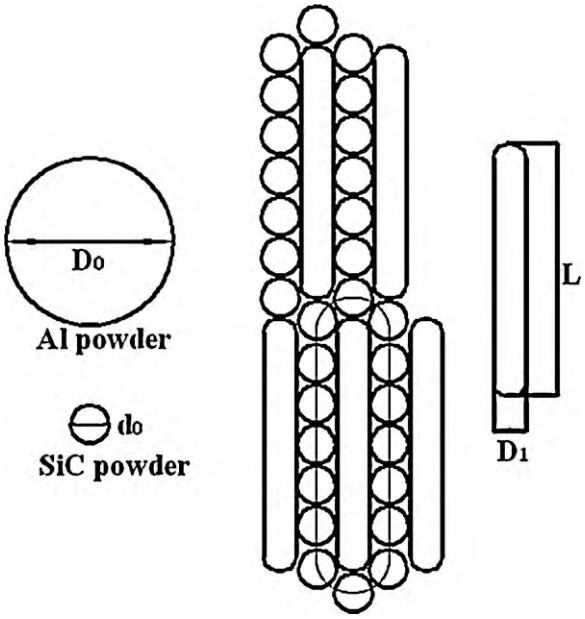

Fig. 11. Schematic of rod model in as-extruded composite. The rods denote deformed aluminum particles after extruding.

shape of the Al particle changes into a regular rod after extrusion.

(b) The volume of the Al particle does not change during extrusion.

According to invariable volume of the aluminum particles, we can get:

$$\frac{4}{3}\pi\left(\frac{D_0}{2}\right)^3 = \frac{1}{4}\pi {D_1}^2 L \tag{8}$$

where D_1 and L are the diameter and length of the Al powder rod after extrusion, respectively.

The ratio of extrusion γ is equal to the square of equivalent section area ratio:

$$\gamma = \left(\frac{0.874D_0}{D_1}\right)^2 \tag{9}$$

In the rod model, a simple cyclic unit marked by a continuous thin line is chosen for calculation (Fig. 11). The volume of one Al particle is:

$$V_{Al} = \frac{\pi {D_1}^2 L}{4} \tag{10}$$

And the volume of reinforcements per Al particle is:

$$V_{SiC} = \frac{\pi(D_1 + d_0)^2(L + d_0)}{4} - \frac{\pi D_1^2 L}{4} \tag{11}$$

So the critical volume fraction of reinforcement is:

$$V_{critical} = \lambda\frac{\pi(D_1 + d_0)^2(L + d_0)/4 - \pi {D_1}^2 L/4}{\pi(D_1 + d_0)^2(L + d_0)/4} \tag{12}$$

If the SiC_p fractured during mixing, the mean size of the SiC_p after mixing $d_0^\bullet$ should replace d_0. By introducing $\eta = d_0/d_0^\bullet$, we could get:

$$V_{critical} = \lambda\left(1 - \frac{0.667(\eta D_0/d_0)^3}{(0.874\gamma^{-1/2}\eta D_0/d_0 + 1)^2(0.874\gamma\eta D_0/d_0 + 1)}\right) \tag{13}$$

Calculated by Eq. (13),

$$\frac{\partial(V_{critical})}{\partial(\gamma)} > 0(\lambda > 1); \quad \frac{\partial(V_{critical})}{\partial(PSR)} < 0 \tag{14}$$

From Eq. (14), extrusion or high extrusion ratio can increase the $V_{critical}$ of the composite, which is in accord with a previous report [16] and the results as shown in Figs. 4 and 5.

The as-pressed composites in the second group exhibited pronounced clustering when the SiC_p volume fraction was higher than 15 vol.% (Fig. 4), suggesting that the $V_{critical}$ was about 0.15. Substituting the $V_{critical}$ into Eq. (11), λ was calculated to be 0.27, which was consistent with the value calculated from the lamellar model. After the extrusion which had an extrusion ratio of 9 as shown in Fig. 5, obvious clusters did not appear until the volume fraction of SiC_p was increased to 20 vol.%. The $V_{critical}$ was calculated to be 19 vol.% by Eq. (13), which was close to 20 vol.%. It indicates that the model was in good agreement with the experimental results.

It should be mentioned that the Slipenyuk model was expressed by the following equation [14]:

$$V_{critical} = 0.18\left(1 - \frac{(D_0/d_0)^3}{(\gamma^{-1/2}D_0/d_0 + 1)^2(\gamma D_0/d_0 + 1)}\right) \tag{15}$$

By using the Slipenyuk model, the $V_{critical}$ of the as-extruded composites in the second group of composites was calculated to be 12 vol.%. Clearly, the $V_{critical}$ value was significantly underestimated compared to that estimated from Fig. 5 ($V_{critical} \sim 20$ vol.%) and calculated by Eq. (13) (~19 vol.%). In view of the $V_{critical}$ calculation results, our modified model was more suitable for evaluating the distribution homogenization of reinforcement in the particle reinforced composites.

By introducing $S = D_1/L$ (ratio of diameter to length in the extruding rod model) into Eq. (13), Eq. (13) can be reformed to Eq. (16) which takes the same form as Eq. (6) in the lamellar model.

$$V_{critical} = \lambda\left(1 - \frac{0.667(\eta D_0/d_0)^3}{(1 + 0.874S^{-2/3}\eta D_0/d_0)(1 + 0.874S^{1/3}\eta D_0/d_0)^2}\right) \tag{16}$$

Table 3
Evaluation of reinforcement distribution by extruding or milling in some reported composites.

Composition	PSR	γ	S[a]	V_f (vol.%)	$V_{critical}$ (vol.%)	Actual distribution[b]	Source
2124Al + SiC	28.4	16	–	10	7	Poor	[24]
7xxxAl + SiC	3.4	21	–	20	23	Fair	[25]
	1.43	21	–	20	26	Good	
6061Al + SiC	20	30	–	17.5	12	Poor	[26]
Al + Al_2O_3	560	36	–	1	0.5	Fairly	[27]
				4		Poor	
Al + VC	25	–	36	5	9	Good	[28]
6061Al + Si_3N_4	3.84	–	14	5	5	Good	[20]

[a] The value of S was not from direct results of the references. We first got the value of width of flaky particles in lamellar structure in SEM or OM graphs, then we calculated S from invariant volume of aluminum particles.

[b] Good: homogeneous; Fairly: uniform but some local inhomogeneous; Poor: severely inhomogeneous.

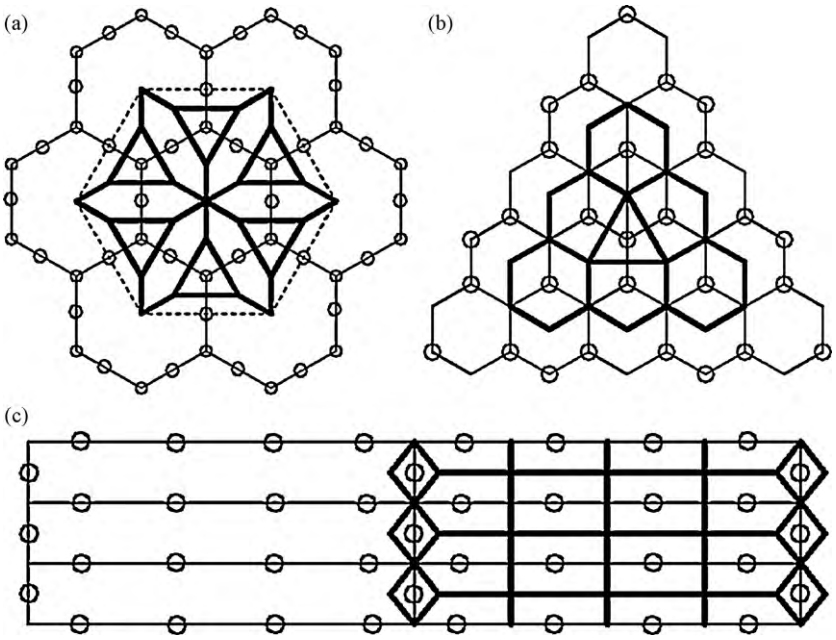

Fig. 12. Schematic of three ideal structures: (a) necklace structure with large PSR, (b) necklace structure with small PSR, (c) lamellar structure of Al with a size ratio of 4:1. Small circles stand for SiC, hexagon in (a), (b) and rectangle in (c) adhered by small circles refer to aluminum. The bold lines crossing Al matrix and containing SiC are meshes generated by Dirichlet Tessellation method.

Eq. (16) indicates that the SiC distribution is closely related to the PSR and S during mixing or extrusion. Small PSR or large deformation of the Al particles contributes to a large $V_{critical}$ and results in a uniform distribution of reinforcement.

The reinforcement distributions in a number of Al matrix composites, reported by other researchers, were also evaluated using Eq. (16). The results are shown in Table 3. For most composites, if the volume fraction of the SiC_p was smaller than the $V_{critical}$, a fair or good distribution was observed, otherwise a poor distribution occurred. These results provide strong supports for the above model.

4.3. Ideal model statistic analysis by Dirichlet Tessellation

Previous discussions were based on the hypothesis that a large critical volume fraction resulted in a more uniform distribution of the reinforcement. In order to investigate the relationship between critical volume fraction and uniformity of reinforcement distribution, three ideal common distribution modes are created (Fig. 12). The first mode is the necklace distribution with a large PSR, the second is the necklace distribution with a small PSR and the third is the streamline-like distribution corresponding to the as-pressed composites fabricated by modified mixing processes or the as-extruded composites.

All of the subjects are restricted to a 2D space, the fraction and size of reinforcements are same, and the areas of the aluminum particles in Fig. 12(a) and (c) are equal. In the first mode, the aluminum particles are set a size of D_0. In the second mode, the aluminum particles are set a size of $D_0/2$. In the third mode, the aluminum particles are set an aspect ratio of 4:1. Numbers of SiC_p in a cyclic unit for all the modes are 5. The dirichlet tessellations [12,23] are meshed in the simplest cyclic unit.

A large COV(A) value, which is the ratio of standard deviation to the mean area of the tessellations, indicates non-homogeneous tendencies [12], and vice versa.

For the necklace distribution with a large PSR shown in Fig. 12(a), COV(A) = 0.49;
For the necklace distribution with a small PSR shown in Fig. 12(b), COV(A) = 0.267;
For the streamline-like distribution shown in Fig. 12(c), COV(A) = 0.237.

From the simple analysis, a small PSR, a modified mixing process or an extrusion corresponding to larger $V_{critical}$ resulted in a more homogeneous distribution of reinforcement, which is in agreement with the hypothesis that a large critical volume fraction of reinforcement could result in homogeneous distribution of reinforcement. In summary, the critical volume fraction model could reflect the influence of the distribution mode on the uniformity of reinforcement distribution, which could also be well explained by the analysis on basis of the Dirichlet Tessellation method.

5. Conclusion

From the results of the present investigation, it can be concluded that the SiC necklace structure could be eliminated and the reinforcement particle distribution could be improved by increasing the BCR, decreasing the PSR, or performing extrusion.

A homogeneous SiC distribution could improve the tensile properties of the composites and the UTS was more sensitive to clusters than the YS.

A critical volume fraction model, which considered the deformation of the aluminum powders and the fracture of the SiC_p during mixing or extrusion, was built to quantitatively evaluate the homogeneity of the SiC_p distribution. Large deformation of aluminum powders or a small PSR could enlarge the value of critical volume fraction of reinforcement, which then led to a more homogenous distribution of SiC_p.

References

[1] D.B. Miracle, Compos. Sci. Technol. 65 (2005) 2526–2540.
[2] M. Rosso, J. Mater. Proc. Technol. 175 (2006) 364–375.
[3] I.A. Ibrahim, F.A. Mohamed, E.J. Lavernia, J. Mater. Sci. 26 (1991) 1137–1156.

[4] J.M. Torralba, C.E. da Costa, F. Velasco, J. Mater. Proc. Technol. 133 (2003) 203–206.
[5] R. Angers, M.R. Krishnadev, R. Tremblay, J.F. Corriveau, D. Dub, Mater. Sci. Eng. A 262 (1999) 9–15.
[6] J.J. Lewandowski, C. Liu, W.H. Hunt Jr., Mater. Sci. Eng. A 107 (1989) 241–255.
[7] S.F. Corbin, D.S. Wilkinson, Acta Metal. Mater. 42 (1994) 1311–1318.
[8] I.C. Stone, P. Tsakiropoulos, Mater. Sci. Eng. A 189 (1994) 285–290.
[9] P.B. Prangnell, S.J. Rodnes, S.M. Roberts, P.J. Withers, Mater. Sci. Eng. A 220 (1996) 41–56.
[10] M. Geni, M. Kikuchi, Acta Mater. 46 (1998) 3125–3133.
[11] A. Borbely, H. Biermann, O. Hartmann, Mater. Sci. Eng. A 313 (2001) 34–45.
[12] J. Boselli, P.J. Gregson, I. Sinclair, Mater. Sci. Eng. A 379 (2004) 72–82.
[13] A. Slipenyuk, V. Kuprin, Y. Milman, J.E. Spowart, D.B. Miracle, Mater. Sci. Eng. A 381 (2004) 165–170.
[14] A. Slipenyuk, V. Kuprin, Y. Milman, V. Goncharuk, J. Eckert, Acta Mater. 54 (2006) 157–166.
[15] V.V.B. Prasad, B.V.R. Bhat, Y.R. Mahajan, P. Ramakrishnan, Mater. Sci. Eng. A 337 (2002) 179–186.
[16] V.V. Bhanu Prasad, B.V.R. Bhat, P. Ramakrishnan, Y.R. Mahajan, Scr. Mater. 43 (2000) 835–840.
[17] M.J. Tan, X. Zhang, Mater. Sci. Eng. A 244 (1998) 80–85.
[18] A. Bhaduri, V. Gopinathan, P. Ramakrishnan, A.P. Miodownik, Mater. Sci. Eng. A 221 (1996) 94–101.
[19] J.B. Fogagnolo, E.M. Ruiz-Navas, M.H. Robert, J.M. Torralba, Scr. Mater. 47 (2002) 243–248.
[20] J.B. Fogagnolo, F. Velasco, M.H. Robert, J.M. Torralba, Mater. Sci. Eng. A 342 (2003) 131–143.
[21] J. Abenojar, F. Velasco, M.A. Martisez, J. Mater. Proc. Technol. 184 (2007) 441–446.
[22] K. Hanada, Y. Murakoshi, H. Negishi, T. Sano, J. Mater. Proc. Technol. 63 (1997) 405–410.
[23] S. Ghosh, Z. Nowak, K. Lee, Acta Mater. 45 (1997) 2215–2234.
[24] M.K. Jain, V.V. Bhanu Prasad, S.V. Kamat, A.B. Pandey, V.K. Varma, B.V.R. Bhat, Y. Mahajan, Int. J. Powder Metall. 29 (1993) 267–275.
[25] J.J. Lewandowski, C. Liu, W.H. Hunt Jr., in: P. Kumar, al. et (Eds.), Processing and properties for Powder Metallurgy Composites, TMS/AIME, Warrendale, PA, 1987, pp. 117–139.
[26] T.G. Nieh, T. Imai, J. Wadsworth, S. Kojima, Scr. Metall. Mater. 31 (1994) 1685–1690.
[27] Y.C. Kang, S.L.I. Chan, Mater. Chem. Phys. 85 (2004) 438–443.
[28] J.B. Ruiz-Naras, Fogagnolo, Composite A 37 (2006) 2114–2120.